ARCHEOLOGICAL SITE DOCUMENTATION AND MONITORING OF CHANGES USING SURFACE-BASED PHOTOGRAMMETRY

Shahaf Levin, Sagi Filin

Transportation and Geo-Information Eng., Technion – Israel Institute of Technology, Haifa 32000, Israel
{shahafl, filin}@technion.ac.il

Commission V, WG 2

KEY WORDS: Close range photogrammetry, surfaces, modeling

ABSTRACT:

Image-based change detection concerns translation of two-dimensional intensity data into three-dimensional changes. The challenges that such analysis offers dictate in many cases imposition of constraints on the camera placement and illumination conditions. Evaluation of changes is then carried out either via point-to-point differencing or via segmentation and classification of the data. Overcoming these limitations, this paper proposes a three-dimensional image-based change detection model that integrates the stochastic nature of the observations into the analysis. In order to relax the need for fixed reference points that are marked in advance, a requirement that cannot always be fulfilled, the paper addresses also the registration of images from different epochs. For registration we propose a surface based alignment model and show that using this scheme, the registration and consequent change documentation can be viewed as two sides of the same problem. Change-detection is then carried out via outlier-detection analysis associated with geodetic network design and measurement. The paper discusses the application of proposed model for the documentation of an archeological excavation site. Results show the applicability of the model as well as its suitability for feature extraction.

1. INTRODUCTION

The need to monitor and document changes within a scene is vital to many applications and many disciplines. Changes may appear in different scales, ranging from significant ones, e.g., removal or introduction of objects, to barely noticeable ones such as object deformation. Using image data, detection methods tend to analyze intensity variations. Radke and Roysam (2005) analyze preprocessing algorithms aiming at filtering "unimportant" changes while maintaining "significant" ones that relate to actual modifications in the scene. The focus is on illumination-invariant algorithms and statistical hypothesis tests. However, changes in the camera position are likely to lead to perspective changes that may turn intensity-driven methods unsuitable.

Point-cloud based change detection is another active research field. Vu et al. (2004) propose an autonomous method for airborne laser scanning driven change detection. Differences between "pre" and "post" grids are computed, and changes are detected according to their distance from the mean value in a difference histogram. Vogtle and Steinle (2004) propose a change detection methodology for urban areas that have undergone disastrous events. Instead of a naïve DSM difference computation, region growing and segmentation procedures are applied to detect buildings, followed by comparison of their parameters. Lindenbergh and Pfeifer (2005) propose a segmentation-based approach when using terrestrial laser scanner. Following the segmentation, test statistics are applied to identify changes. Zeibak and Filin (2007) address change detection when scanners are placed at general locations and propose use of range panoramas to account for variations in scale and viewing.

Using photogrammetry, Ladstaedter and Kaufman (2004) detect changes along a mountain slope via terrestrial images. The authors subtract image derived DTMs that were acquired from a fixed camera position at different epochs. Habib et al. (2001) present a surface-matching based change detection which is based on a point-to-surface registration. Points that do not correspond to the surface following the registration are declared changes. Point-to-object differences are being defined by using an external threshold value, ignoring the stochastic nature of the observations.

The application of terrestrial photogrammetry for site documentation and reconstruction is widely known. Its attractiveness relates to the ease of data collection, low cost and availability of the imaging devices, ability to avoid physical contact with the mapped objects, and the existence of well-established methodologies for the documentation. In this regards, close-range photogrammetry can be considered optimal for change detection. However, when datasets are collected at different epochs and the site has been modified, a point-to-point correspondence cannot be readily assumed, and if fixed control points do not exist, point-based photogrammetry may become complex to apply. In such cases, surface-based models (e.g., Ebner and Strunz, 1988; Jaw, 2000; Schenk, 2000), which offer a more relaxed demand for correspondence between image data and object space, has the potential to offer a more suitable solution.

We present in this paper a surface based block-alignment model and its consequent application to change documentation from close-range images. In order to avoid constraining the camera placement at the time of imaging, the model accounts for the fact that in addition to the detection of changes, registration of the data must be solved. Imaging from general positions implies that resolution differences associated with photogrammetrically extracted data may also exist. Detection of changes is based on outlier analysis. The paper demonstrates the application of the proposed model on an archeological site, where ongoing documentation during excavation was needed. Results show

how the detection model performs well, and can also be utilized for feature extraction.

2. SURFACE-BASED CHANGE DETECTION MODEL

The proposed model is based on surface-based image registration and utilizes outlier detection methodologies to identify changes between epochs. Outlier detection is discussed first, followed by presentation of the proposed registration model and the derived change-detection scheme.

2.1 Outlier detection

Outliers are defined as observations which disagree with a given model. Several methods associated with least-squares estimation have been proposed for their detection, and are analyzed herein. The common ones among them include Baarda's data-snooping (Baarda, 1968), the Tau-test, and Danish method (Berberan, 1992).

Data-snooping is rooted in probability theory and utilizes hypothesis tests. The null hypothesis considers the existence of no outliers while the alternative considers the existence of only one gross error. In practice, data snooping allows detection of multiple outliers in an iterative fashion. Its underlying assumption is that the a priori standard deviation (*std.*) of a unit-weight observation, σ_0, is known, thereby enabling to calculate the standard deviation of the residuals. Normalized residuals u_i are calculated via

$$u_i = \frac{|v_i|}{\sigma_0 \sqrt{q_{v_i v_i}}} \tag{1}$$

with v_i, the residual of the i-th observation and $q_{v_i v_i}$, the element in the cofactor matrix of the observation corresponding to that observation. u_i is used as the test value for the hypothesis test, with $u_{\alpha 0}$ the critical value (usually taken from nomograms). If the test value exceeds the critical value, the corresponding observation is considered an outlier and discarded from the dataset.

The Tau-test method is similar to the data snooping, but does not assume that σ_0 is known. Instead, the a posteriori *std.*, $\hat{\sigma}_0$, is used to calculate the normalized residuals and the test value T_i. The normalized residuals, u_i^{τ}, are calculated via

$$u_i^{\tau} = \frac{|v_i|}{\hat{\sigma}_{v_i}} = \frac{|v_i|}{\hat{\sigma}_0 \sqrt{q_{v_i v_i}}} \tag{2}$$

Since v_i and $\hat{\sigma}_0$ are statistically dependent, the *t*-distribution does not apply here, and u_i^{τ} is governed by the τ-distribution. Tables listing the τ-distribution are not easily accessible; however, the critical value can be calculated based on *t*-distribution values via

$$\tau_f = \frac{t_{f-1}\sqrt{f}}{\sqrt{f - 1 + t_{f-1}^2}} \tag{3}$$

with *t*, the *t*-distribution value and *f*, the degrees of freedom. Similar to Baarda's test, if the test value exceeds the critical value the corresponding observation is considered as an outlier discarded from the dataset. Only a one outlier can be detected at a time.

Both data-snooping and the tau-test assume that only one outlier exists, thus their underlying theoretical foundations cannot be readily applied if more than a single outlier exists. Even though multiple outliers can be iteratively detected, one at a time, utilizing them for the detection of multiple outliers, as change-detection cases offer, may prove difficult.

Robust estimation methods for outlier detection are purely heuristic, making no assumption about the stochastic nature of the observations. They are founded on the assumption that large residuals relate to less accurate observations and vice-versa. Therefore, after performing the least-squares estimation, the a priori weights of the observation are replaced with functions of the residuals and the model is estimated again. This process is carried iteratively until convergence is reached.

Several reweighting functions exist, with the one applied by the Danish method having the form

$$p_{\nu+1} = \begin{cases} p_\nu & u_i^D \le c \\ p_\nu \cdot \exp\left(-\frac{u_i^D}{c}\right) & \text{otherwise} \end{cases} \tag{4}$$

with, $\nu = 1, 2, \ldots$ the iteration number, p_ν the weight on the ν^{th} iteration, u_i^D the normalized residual

$$u_i^D = \frac{|v_i|}{\hat{\sigma}_0}\sqrt{p_1} \tag{5}$$

p_1 is the observation weight at the first iteration, and *c* a critical value which is usually set in the range of 2-3. Following the model's convergence, all residuals with values greater than a given threshold are considered outliers. Two options can be taken to handle them. The first is removing outlying observations and solving the model without them. The second is using the final estimation of the Danish method as the final weights for the outliers which should be close to zero and not affect the quality of the solution.

The reweighting function can wear a variety of forms. As an example, Huber (1981) proposes

$$p_{\nu+1} = \begin{cases} p_\nu & u_i^A \le c \\ p_\nu \cdot \frac{1}{u_i^A - (c-1)} & \text{otherwise} \end{cases} \tag{6}$$

with u_i^A given in Eq. (5).

It should be noted that for the underlying robust-estimation-methods assumption to hold true, namely large residuals indicate less accurate observations, an estimation model with high-internal reliability should be used. Such models are characterized by high redundancy numbers, meaning that most of the observations error is absorbed in its respective residual.

2.2 Image registration using surfaces

Surface-based image registration can apply only for a set of two images or more. This observation can be deduced when comparing the number of observations to the number of unknowns. It suggests that photogrammetric surface-based registration should have a notion of associating two 3D reference frames. Such relation may translate into similarity transformation based registration. The need to determine 3D coordinates necessitates extraction of homologous point from the images. For reliable detection of changes, a dense photogrammetric set of points may be required. Obtaining such

set, an autonomous method for the extraction of homologous points is introduced.

2.2.1 Homologous point extraction

Several algorithms exist for extraction of homologous points in an image set, e.g., cross-correlation and least-squares matching, to name a few (Schenk, 2000). These methods perform well when no substantial change exists between the image sets, as in the case of aerial photographs and short baseline stereo-pairs. However, when substantial perspective changes exist between images, as may happen with close-range imaging, these methods may fail to produce reliable matches. In contrast, the Scale-Invariant-Feature-Transform (SIFT) (Lowe, 2004) is designed as invariant to scale, rotation, and illumination, while in practice it also exhibits some level of invariance to perspective changes. The SIFT methodology consists of: i) detection of candidate interest points via scale-space extrema search, ii) localization of the keypoints, iii) orientation assignment based on the image local gradient to ensure scale and orientation invariance, and iv) descriptor computation. For each detected keypoint a descriptor which is invariant to scale, rotation and changes in illumination, is generated. The descriptor is based on orientation histograms in the appropriate scale. Each descriptor consists of 128 values.

The extraction of candidate counterpart points is vital in the present case for two purposes: the first is the establishment of the relative orientation between image pairs, and the second is launching the point-to-surface registration model. These two goals have two different objectives, the first is obtaining a reliable set of points for orientation where the focus is on their quality, and the second is obtaining a detailed surface model, with focus on quality but also on their quantity. In this regards, the ability to control the amount of keypoints extracted by the SIFT model provides an excellent and efficient means for the provision of large set of potential 3D points. Therefore, the counterpart extraction process is applied here in two phases.

For the relative orientation, a high filtering threshold is set, so that only a marginal number of outliers result. Considering the fact that for the computation of the relative orientation only five points are required, setting a high threshold still provides a great number of degrees of freedom than what is customary to use.

The computed relative orientation also defines the geometrical locus where all candidate counterparts of a given point can be found. Therefore, for the second phase that concerns describing the surface, the initial filtering threshold value for potential corresponding points is decreased. Matches are not only evaluated by their descriptor similarity, but also by their proximity to the epipolar line in the second image. Proximity is computed by image distance between a point and the epipolar line it is expected to lie on. Points whose distances exceed a certain threshold value are discarded. The distance is a function of the accuracy of the estimation of the relative orientation. Notice that outlying matches that lie along epipolar lines cannot be detected and will be identified as changes in by the change-detection scheme.

2.2.2 Surface-based registration model

With the extraction of 3D pointsets, the registration of both datasets can be performed. The registration process objective is to align datasets from different epochs while enabling easy identification of outlying observations. Registration of 3D datasets requires relating entities between both datasets. Besl and McKay (1992) propose computing a rigid-body transformation in an iterative fashion by updating correspondence. Convergence is reached when the actual matches are found. Chen and Medioni (1992) proposed a point-to-surface registration scheme for determining the rigid body transformation. Parameters are based on minimizing the sum of square-distances between a pointset and a surface. Grün and Akca (2005) add a scale factor to the algorithm.

In order to accommodate the settings that close-range photogrammetry offer, namely, occlusions, and varying scale and resolution, a point-to-surface model is adopted. In this scheme, one epoch is described as a pointset, and the other has the form of a surface-model. The datasets alignment is implemented by determining the similarity transformation between the reference coordinate systems of both epochs, namely

$$\mathbf{p} = m \cdot \mathbf{R} \cdot (\mathbf{p}' - \mathbf{t}) \tag{7}$$

with **p'** a point in the first (*point*) epoch reference coordinate system, **p** a point in the second (*surface*) epoch reference coordinate system, **t** the translation between the two systems, **R** the orthonormal rotation matrix, and *m* the scale factor.

The common surface models are usually provided either in the form of a regular-grid or by a set of irregularly distributed points. For the latter case the triangular-irregular-network (TIN) is usually established as a surface representation. Regular grids are easy to generate, manipulate, and access, however they are limited to 2.5D, and by nature apply only for regular data. The TIN representation is more general than the regular grid model, more flexible, and can be employed to a full 3D model as well. The common use of the TIN representation and its greater flexibility, motivate the formulation of the solution using this representation.

The local TIN surface patches, defined by the three triangle vertices, are considered planar. The point-to-plane distance δ_i can then be written in vector form is

$$\delta_i = \begin{bmatrix} \mathbf{n}_i^T & d_i \end{bmatrix} \cdot \begin{bmatrix} \mathbf{p}_i \\ 1 \end{bmatrix} \tag{8}$$

with $\mathbf{n}_i = [n_i^x, n_i^y, n_i^z,]^T$ the normalized (unit length) normal vector to the plane defined by triangle t_i, d_i the plane constant, and $\mathbf{p}_i = [x_i, y_i, z_i]$. Linking Eq. (6) and Eq. (7) leads to

$$-m\mathbf{n}_i^T\mathbf{R}\mathbf{t} + m\mathbf{n}_i^T\mathbf{R}\mathbf{p}_i' + d_i - \delta_i = 0 \tag{9}$$

The quantities in Eq. (9) can be categorized as belonging into unknowns and observations. $\mathbf{s} = [t_x, t_y, t_z, m, \omega, \phi, \kappa]^T$ is the vector of unknown transformation parameters, **p'** is the observation for the first epoch, **n** and *d* are the observations derived for the epoch, and δ, is the observation for the difference between the two epochs. A strong dependency exists between **p'** and [**n**, *d*] through δ. Modeling this dependency is impractical, and since the interest of the proposed model is to estimate the differences between datasets, **p**', **n**, and *d* are considered constants. Eq. (9) is nonlinear, thus in order to perform a least-squares estimation, linearization using Taylor series expansion leads to

$$\mathbf{A}\mathbf{s} + \mathbf{B}\mathbf{v}_\delta + \mathbf{w} = 0 \tag{10}$$

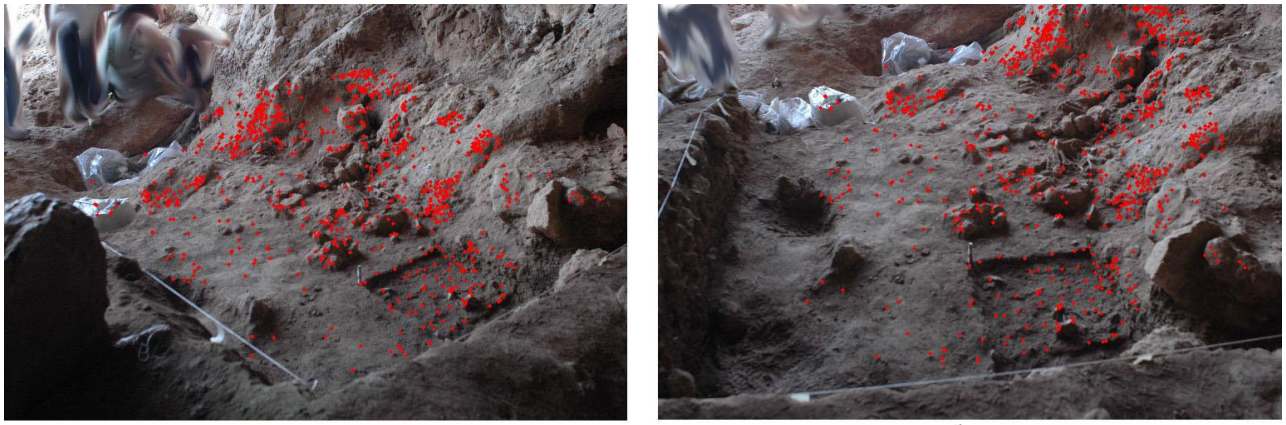

Figure 1. The first epoch image-pair, a) the left image, b) the right image. Corresponding points extracted using the SIFT algorithm are marked in red.

with **s** the differential correction to the initial transformation parameters approximations, and $\mathbf{v}_\delta$ the residuals of the distance observations, and

$$\mathbf{A} = \frac{\partial f(\mathbf{S}, \mathbf{p}, T)}{\partial \mathbf{S}} \quad ; \quad \mathbf{B}_p = \frac{\partial f(\mathbf{S}, \mathbf{p}, T)}{\partial \delta} = -\mathbf{I}$$

The least-squares target function becomes then

$$\mathbf{s}^T\mathbf{P}_s\mathbf{s} + \mathbf{v}_\delta^T\mathbf{P}_\delta\mathbf{v}_\delta - 2\mathbf{k}^T(\mathbf{A}\mathbf{s} - \mathbf{v}_\delta + \mathbf{w}) = \min \tag{11}$$

with $\mathbf{P}_\delta$ the weight matrix for the observations, $\mathbf{P}_s$ the weight matrix for the initial values of the unknowns, and **k** the vector of Lagrange multipliers. Unless prior knowledge about the relation between the two datasets exists, $\mathbf{P}_s$ is usually set to zero. Solving Eq. (10) leads to

$$\hat{\mathbf{s}} = -\mathbf{N}^{-1}\mathbf{A}^T\mathbf{P}_\delta\mathbf{w} \tag{12}$$

$$\hat{\mathbf{v}}_\delta = \mathbf{A}\hat{\mathbf{s}} + \mathbf{w} \tag{13}$$

with $\mathbf{N} = \mathbf{A}^T\mathbf{P}_\delta\mathbf{A} + \mathbf{P}_s$. The a posteriori variance is given by

$$\hat{\sigma}_0^2 = \frac{\hat{\mathbf{s}}\mathbf{P}_s\hat{\mathbf{s}}^T + \hat{\mathbf{v}}_\delta\mathbf{P}_\delta\hat{\mathbf{v}}_\delta^T}{n-u} \tag{14}$$

with *n* the number of condition equations (equals to the number photogrammetric model points), and *u* the number of transformation parameters (seven here).

The initial registration procedure assumption is of no changes between epochs, so that all observations are inliers. This assumption is equivalent to the null hypothesis tests. Since both datasets represent the same object, the value δ is set to zero. Setting the values in the weight matrices is discussed in the following.

Testing the proposed model using various simulated and real world configurations shows that redundancy numbers of 0.7-0.9 are constantly achieved, almost irrespective of the configurations. These considerably high values are well suited for detection of outliers.

The discrete, piecewise, representation of the surface by the TIN model requires establishing a correspondence between the points and the triangles. The model associates points to a triangle via the two following conditions: *i*) the point is inside the triangle – a vector from the point to the triangle, with direction parallel to the normal to the triangle plane, intersect the triangle plane inside of it, and *ii*) the distance between the point and the triangle plane is the minimal with respect to all triangles that fulfill the first condition.

2.3 Change-detection scheme

Aiming for a method that can handle, simultaneously multiple disagreements within the entire dataset, both data-snooping and the tau-test which seek only one outlier at a time are discarded. The robust estimation driven method is therefore applied. The procedure follows the scheme:

1. Setting initial weights in $\mathbf{P}_\delta^0$.
2. Solving the registration model with the current $\mathbf{P}_\delta^\nu$ (with ν the iteration number).
3. Calculating new weights according to Eq.(4) and setting $\mathbf{P}_\delta^{\nu+1}$. *c* is set at the range of 1.5-3, depending on the quality of the data.
4. If $\mathbf{P}_\delta^{\nu+1}$ differ from $\mathbf{P}_\delta^{\nu+1}$ go to stage 2.
5. Declare all observation with residual higher than a threshold value as changes.

The initial values in $\mathbf{P}_\delta^0$ are set according to the expected accuracy of the 3D points that were reconstructed from the photogrammetric models. Generally, they should be close to unity. Areas in the datasets (both epochs) with questionable accuracy or reliability should yield lower weights, which should be taken in consideration in the final stage of the procedure. It is noted that for the actual detection of change, estimation of the registration parameters $\hat{\mathbf{s}}$ may not be of great interest, and so Eqs. (12) and (13) can be combined to estimate the residuals vector only via

$$\mathbf{v}_\delta = \left(-\mathbf{A}\mathbf{N}^{-1}\mathbf{A}^T\mathbf{P}_\delta + \mathbf{I}\right)\mathbf{w} \tag{15}$$

In the final step, when changes are identified, one should take into considerations observations with initial low weights. These will inherently have large residuals regardless of the existence of an actual change. If these initial weights are below a threshold value (the weight corresponding to the residual size

a **b**

Figure 2. Changes between epochs (a) shows the results of the change-detection procedure, green points indicate correct detections, yellow misclassified changes, and red indicate false detections, (b) the reconstructed changes.

($p_{critical} = \hat{\sigma}_0^2 / v_{critical}^2$) for declaring changes, they should be flagged suspicious as they may indicate gross errors during their 3D reconstruction phase.

3. RESULTS AND DISCUSSION

The application of the proposed model is demonstrated on a documentation project in an archeological excavation site (the Raqefet cave; Nadel et al., 2008) in the Carmel mountain ridge, Israel. The study is part of ongoing research on the origins and use of manmade-bedrock-holes in ancient cultures. An excavation campaign performed on August 2008 served as the case study for the analysis. The study was performed on a ~10 m^2 area, and images were acquired using a Nikon D70 camera, with a 24 mm Nikkor lens.

We demonstrate the orientation results on the first epoch where images were acquired with a ~1.5 m base length and convergence angle of ~25^o. Applying the SIFT algorithm on the image set resulted in a set of 913 points that were autonomously extracted. Among them 101 points have passed the high threshold filtering stage (threshold was set to 4) and the rest where found corresponding by limiting the search to the epipolar line locus. Of the 101 points that were used for the relative orientation phase none were outliers. Similar results were observed in other stereo-pairs on which the keypoint extraction model was applied. The set of homologous points is presented in Figure 1, while being marked on the images. The extraction accuracy was ~1.5 pixels and the 3D reconstruction accuracy was 0.5 cm. The dataset of this epoch is represented as a pointset. The site was then imaged again after objects have been removed from the site. Data from that epoch served as the reference and was represented by a TIN surface-model.

Following the relative orientation of images from the two individual epochs, the registration and change-detection scheme were performed. For the orientation, the initial weight matrix for the observation $\mathbf{P}_\delta^0$ was set as an identity matrix. Danish method was used of reweighting and the critical value was set to c = 2. The weight critical value for declaring a change was set to p_{critical} = 0.1, which correspond to a critical residual value of $3\sigma_0$. The results of the change-detection procedure on one of the images are shown in Figure 2a, and their completion into the objects that were removed is highlighted in Figure 2b. Changes that were detected are indicated by green points, changes that were not detected by yellow points and red points indicate points that were falsely detected as changes. Sixty seven points were identified as part of objects that were removed. Sixty four of those points (96%) were successfully identified and only three were not. All the unidentified points were sampled close to ground and therefore are not considered as change. Such points would have been reclassified following cluster analysis. Six points which were not part of a removed object were identified as changes.

Figure 3b shows the weight matrix $\mathbf{P}_\delta$ behaviour throughout the iterations. The mean weights for observations inside and outside of the change area, indicated by solid red and blue lines respectively, clearly show convergence of the detection procedure at the sixth iteration. The dashed black line indicates the critical weight P_{critical} = 0.1. Setting higher values for the critical value c in the re-weighting step (c=2 here) will yield faster convergence, but may lead to more false detections. The dashed blue line indicates the minimal weights for observation in non-changing areas of the site. At the point of convergence the red and dashed-blue lines cannot practically be separated. This is due to the rapid convergence of the exponent function used for weighting used by Danish method.

In an attempt to avoid false detections, the scheme was performed also using the Huber weighting function (Eq. (5)). Out of the 67 existing changes 63 were successfully detected and no false detections were made. The convergence of the procedure was clearly much slower, and was reached only after the eleventh iteration, almost twice slower than Danish methods.

It is noted that the same procedure used for change-detection can be used, with slight modification, for feature extraction assuming that a reference surface model is given. Whereas datasets in the change-detection model are defined temporally, according to their time of acquisition, applying the same model on a coarse surface-model of a site and an unclassified pointset, containing both terrain and objects, will enable detecting "outlying" points with respect to the reference surface-model, thus enabling classifying them as objects or added details.

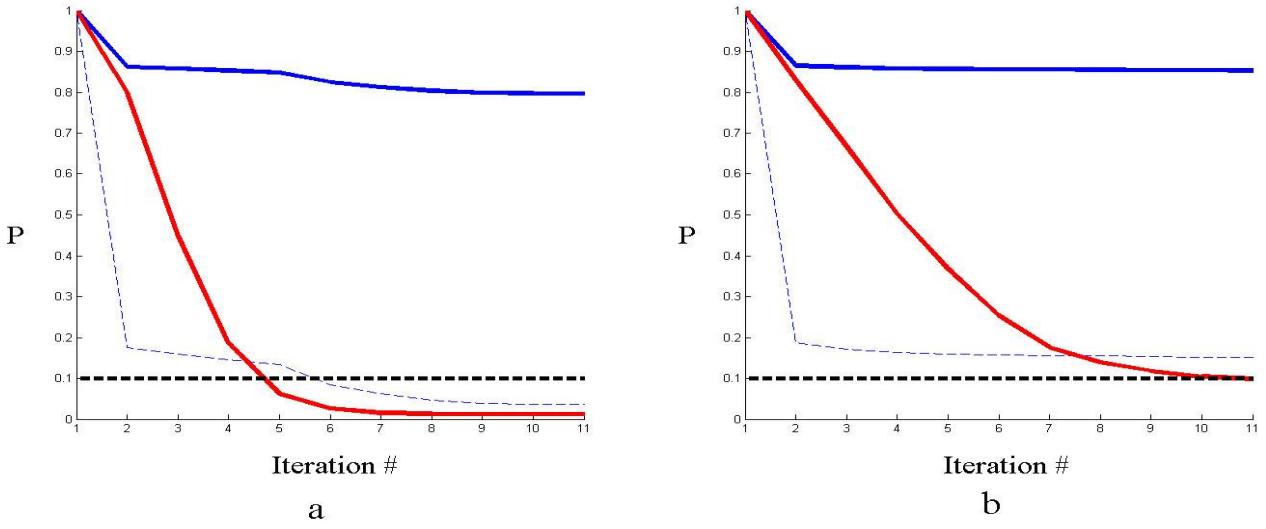

Figure 3. Mean weights as function of iteration number for Danish (a) and Huber (b) methods. Red lines indicate mean weights for observations in changing areas; solid blue lines indicate mean weights for observations in the non-changing areas. Dashed blue lines indicate the minimal weights for observations in the non-changing areas.

4. CONCLUSIONS

This paper has demonstrated the utilization of surface-based photogrammetry as a basis for a robust-estimation change detection model. It has shown how combining the two allow for fast and reliable change-detection in close-range scenes, detecting almost all changes while making only a marginal number of false detections. The use of registration model for change-detection relieves the need for establishing control network, and the use of a surface based model relives the need of identifying corresponding points in the image set. Such models are useful for the documentation changes with no need for lengthy on site procedures.

5. ACKNOWLEDGEMENTS

The research was funded in part by the joint Technion-University of Haifa research fund. The authors would like to thank Dr. Dani Nadel for introducing us to the cave excavation project.

6. REFERENCES

Baarda, W., 1968, A Testing Procedure for Use in Geodetic Networks. *Publ. Geod. New Ser.*, **2**, 27-55.

Berberan, A., 1992. Outlier Detection and Heterogeneous Observations a Simulation Case study. *Aust. J.Geod. Photogramm. Surv.*, **56**, 49-61.

Besl, P. and McKay, N. 1992. A Method for Registration of 3-D Shapes. *Trans. on PAMI*, **14**(2), 239 - 256.

Chen, Y., Medioni, G., 1992.Object modeling by registration of multiple range images. *Image and Vision Computing* **10**(3), 145–155.

Ebner H. and Strunz, G., 1988. Combined Point Determination Using Digital Terrain Models as Control Information. *Int. Archives of Photogrammetry and Remote Sensing*, **27**(B11), III/578-587.

Grün A. and D. Akca, 2005. Least squares 3D surface and curve matching. *ISPRS Journal of Photogrammetry &Remote Sensing* **59**(3), 151–174.

Habib, A., Lee, Y., Morgan, M., 2001. Surface Matching and Change Detection Using the Modified Hough Transform for Robust Parameter Estimation. *Photogrammetric Record*, **17**(98), pp. 303-315.

Huber, P.J., 1981, *Robust Statistics*. Wiley: New York.

Jaw, J. J., 2000. Control Surface in Aerial Triangulation. *International Archives of Photogrammetry and Remote Sensing*. **33**(3B).

Ladstaedter, R., Kaufmann, V., 2005. Change Detection of A Mountain Slope by Means of Ground-Based Photogrammetry: A Case Study in The Austrian Alps. *4th ICA Mountain Cartography Workshop.*

Lindenbergh, R., Pfeifer, N., 2005. A Statistical Deformation Analysis of Two Epochs of Terrestrial Laser Data of A Lock. *In Proceedings of the 7th Conference on Optical 3- D measurement techniques*, Vienna, Austria. pp. 61-70

Lowe, D.G. 2004. Distinctive Image Features from Scale-Invariant Keypoints. *International Journal of Computer Vision.* **60**(2), pp. 91-110.

Nadel, D., G. Lengyel, F. Bocquentin, A. Tsatskin, D. Rosenberg, R. Yeshurun, G. Bar-Oz, D.E. Bar-Yosef M., R. Beeri, L. Conyers, S. Filin, I. Hershkovitz, A. Kurzawska and L. Weissbrod. 2008. The Late Natuafian at Raqefet Cave. Journal of the Israel Prehistoric Society. 38: 59-131.

Radke, R., Roysam, B., 2005. Image Change Detection Algorithms: A Systematic Survey. *IEEE Transactions on image processing*. 14(3).

Schenk ,T., 2000. Digital Photogrammetry, Volume I: Background, Fundamentals, Automatic Orientation Procedures. Terra Science.

Vögtle, T., Steinle, E., 2004. Detection and Recognition of Changes In Building Geometry Derived From Multitemporal Laserscanning Data. *In Proceedings of the XXth ISPRS Congress*. July 12-23, 2004 Istanbul, Turkey. pp. 428-433.

Vu, T., Matsuoka, M., Yamazaki, F., 2004. LIDAR-Based Change Detection of Buildings in Dense Urban Areas. *IEEE International Geoscience and Remote Sensing Symposium (IGARSS '04).*

Zeibak, R., Filin, S., 2007. Change detection via terrestrial laser scanning. *International Archives of Photogrammetry and Remote Sensing*. **36**(3/W52): 430-435.